

## Analytical approach to the linear $E \otimes e$ Jahn-Teller problem

Janette L. Dunn and Mark R. Eccles

*School of Physics and Astronomy, University of Nottingham, University Park, Nottingham, NG7 2RD, United Kingdom*

(Received 26 February 2001; revised manuscript received 29 June 2001; published 15 October 2001)

The  $E \otimes e$  Jahn-Teller effect has been studied previously by many authors. This system is important because, as well as providing results that are useful in their own right, such as for modeling experimental data, it is a relatively simple system that can be used to test ideas before applying them to more complicated systems. The most notable feature of this system is that in linear coupling, the lowest adiabatic potential energy surface forms a two-dimensional trough. Vibrations across the trough and rotations around the trough must both be taken into account. Previous analytical approaches to this system give results that differ by a factor of 2 from numerical results in strong coupling. These approaches are also difficult to extend to more complicated systems. In this paper, we develop an analytical method that shows how the approach can be extended to other systems. We also eliminate the factor of 2 discrepancy by including coupling to the upper potential sheet. Finally, we show that a reasonable approximation to the true linear coupling results can be obtained by including only those points on the trough that become minima when weak quadratic coupling is added to warp the trough, as long as anisotropy in the resultant wells is taken into account.

DOI: 10.1103/PhysRevB.64.195104

PACS number(s): 71.70.Ej

### I. INTRODUCTION

Electron-phonon coupling, via the so-called Jahn-Teller (JT) effect, can have a significant influence on the energy levels and wave functions of a wide variety of systems. The most widely studied vibronic systems are those in cubic symmetry. This symmetry applies to many systems in nature, such as substitutional magnetic ion impurities in III-V and II-VI semiconductors and various fluoride and chloride crystals. Cubic symmetry is also amongst the simplest to deal with. This means that it is ideal for developing theories that can later be applied to more complex systems, such as the icosahedral symmetry that is applicable to fullerenes and various biological molecules.

It is important to have good theoretical descriptions of JT systems because this provides information on the energy levels and vibronic states that can then be used to model specific systems in order to interpret experimental data. One important application of these results is for the calculation of JT (or Ham) reduction factors (RF's).<sup>1-3</sup> These are needed to predict the forms of effective Hamiltonians used to model the effect of external perturbations, such as stress or spin-orbit coupling. Compared to the non-vibronic cases, some terms are reduced in magnitude (or even change sign). For example, the orbital contributions to the Zeeman and spin-orbit interaction terms of several transition metal impurity ions are quenched to zero by vibronic interactions.<sup>1</sup> Also, other new terms appear in second-order that will dominate in the effective Hamiltonians when first-order terms are quenched. The general ideas concerning these first and second-order RF's can be found in various books and review articles.<sup>4,5</sup> There are also numerous publications giving details of the calculation of RF's both in specific systems and in more general terms.<sup>6,7</sup>

The cubic JT system that has received the most attention over many years is the  $E \otimes e$  JT system, in which an orbital doublet  $E$  is coupled to  $e$ -type vibrations. In the linear  $E \otimes e$  JT effect, the lowest adiabatic potential energy surface

(APES) contains a continuous two-dimensional trough of minimum energy points, commonly referred to as a "Mexican hat." The motion of the system is then characterized by a vibration across the trough and a rotation around the trough. This picture holds for all coupling strengths except the weak coupling limit. However, real systems are likely to be affected by higher order effects such as quadratic coupling or anharmonicity. These cause the trough to warp to give three low-symmetry minima (or wells). When the barriers introduced are large enough, the motion near the minima can be treated as a pure two-dimensional vibration, although the frequency of vibration in the parallel direction will be significantly lower than in the perpendicular direction. Tunneling between equivalent minima then restores the cubic symmetry. It is desirable to examine the two limiting cases of pure vibration and pure rotation. The results can be compared and deductions made about real systems, which are likely to lie between these two extremes with shallow barriers resulting in a hindered vibration around the trough.<sup>4</sup>

The first numerical results for the energies of the  $E \otimes e$  JT problem were obtained some 40 years ago,<sup>8,9</sup> followed by improvements using more modern computational methods.<sup>10</sup> These approaches can start from either the weak or the strong coupling limit, as reviewed by Pooler.<sup>5</sup> Nevertheless, efforts to produce reliable analytical results are continuing today.<sup>11,12</sup> Analytical results give more physical insight into the problem than numerical results. They also form a basis for further calculations, such as those of RF's, which are not possible with corresponding numerical approaches. Also, analytical methods often naturally lead to extensions to other situations, such as multimode JT problems,<sup>13</sup> or the inclusion of additional perturbations. One example showing the physical insight gained by analytical methods is recent work which has shown that under conditions of very strong quadratic coupling to the  $e$  mode, the ground state of the  $E \otimes e$  system can be an  $A$ -type singlet.<sup>14</sup> Usually, the ground state of a JT system has the same symmetry as the original orbital state. The crossover to a singlet ground state, which has also

been observed for the icosahedral  $H \otimes h$  JT system in strong linear coupling,<sup>15,16</sup> can be understood in terms of different Berry phases around competing tunneling paths.

Various analytical approaches have been employed by different authors. Some apply only to specific ranges of coupling strengths and others work reasonably well for all coupling strengths. Much of the earlier work has been reviewed by a number of authors.<sup>2,4,5</sup> One approach to the  $E \otimes e$  problem is to treat the states in the wells as displaced harmonic oscillators using Glauber states,<sup>17,18</sup> using ideas developed earlier by Judd,<sup>19</sup> and by Judd and Vogel,<sup>20</sup> and further discussed by Barentzen *et al.*<sup>21</sup> The Glauber state approach has also been applied to the specific example of  $\text{Fe}^{2+}$  ions in ZnTe and ZnS.<sup>22</sup> General expressions for the matrix elements of all  $\Gamma \otimes e$  JT systems, including the  $E \otimes e$  problem, have been obtained from group theoretical arguments.<sup>23</sup> Variational approaches have also been used, both for the basic  $E \otimes e$  problem<sup>24–26</sup> and for the related pseudo JT effect.<sup>27</sup> Other methods include operator techniques<sup>12</sup> and an analytical series approach.<sup>28</sup> Nonadiabatic contributions have also been investigated.<sup>11</sup> A discussion of the determination of RF's for excited states exhibiting an  $E \otimes e$  JT effect can be found in Fletcher and Stedman.<sup>29</sup>

Of the variety of methods used to solve the linear  $E \otimes e$  problem, the methods based on Glauber states are very attractive because the states obtained are expressed in a simple form that is both easy to understand and easy to use in subsequent calculations. However, one drawback is that in strong (linear) coupling, the calculated energy is larger than the strong-coupling limit of  $-E_{\text{JT}} + \frac{1}{2}\hbar\omega_E$  by twice the expected amount. This effect was first observed by Judd<sup>19</sup> in 1974 in studying the fivefold unitary and rotation groups  $U_5$  and  $R_5$ , when discussing results of O'Brien on the  $T \otimes (e + t_2)$  system.<sup>3</sup> He pointed out that both potential and kinetic energy terms contribute to the rotational term, whereas a "classical" treatment of rotation considers only the kinetic energy. He also noted that the off-diagonal matrix elements that occur when coupling to the upper APES is included have the effect of exactly halving the rotational term and will hence produce the correct energy results. It has also been noted by Chancey<sup>18</sup> that the RFs for the  $E \otimes e$  problem calculated using Glauber states only exhibit the correct strong-coupling behavior when the perturbation calculation is carried out to second-order.<sup>30</sup> However, Chancey<sup>18</sup> did not attempt to correct his Glauber states to take account of this coupling. Another drawback of the Glauber state methods used so far is that it is difficult to see how to extend them to more complicated systems, such as the icosahedral  $T \otimes h$  problem in which the lowest APES forms a three-dimensional trough.

The current authors have developed an analytical method for obtaining well states when quadratic coupling is included by using two unitary transformations. The first transformation is a shift transformation to displace the origin of phonon coordinates to the well positions.<sup>31</sup> The displaced oscillator states obtained for each well are essentially the same as Glauber states, although the origin of their construction is somewhat different. The well states are appropriate to a static JT effect in infinitely strong coupling only. Therefore, tun-

neling between equivalent wells must be introduced to model the dynamic JT effect by taking appropriate linear combinations of the well states. This is most readily achieved using projection operators.<sup>32</sup> This method has been applied to all of the cubic JT systems including  $E \otimes e$ ,<sup>33–35</sup> as well as to icosahedral systems.<sup>36</sup> The main advantage of this approach over many of the other approaches is that the states are in a form that can be readily used for further calculations, such as in the evaluation of JT reduction factors.

The shift transformation results in vibrational frequencies that are the same in all directions, i.e., the wells are isotropic. This is unphysical in trough problems such as  $E \otimes e$ , where shallow barriers in the direction around the trough means that the frequency of vibration in this direction can be expected to be much lower than that across the well. It has been shown that anisotropy can be introduced mathematically by applying a scale transformation in addition to the shift transformation.<sup>37</sup> Symmetry arguments are used to generate different vibrational frequencies in the different symmetry directions. However, this approach has not been applied previously to the  $E \otimes e$  system.

The significant difference between JT problems with a trough in the APES and those with wells is that the rotation(s) around the trough must be taken into account. A method such as the shift transformation can be used to obtain the positions of the points forming the bottom of the trough. However, whereas with wells the correct tunneling states are formed from a linear combination of a small number of equivalent well states, there is now an infinite number of equivalent points to be included. Therefore, the sum must become an integral over the states at all minimum points.

The principal aim of this paper is to develop the transformation and projection operator approach used previously for well problems to take account of the continuous nature of trough problems, utilizing the best aspects of the transformation and Glauber state approaches. The results are applied to the linear  $E \otimes e$  problem. The states obtained for this simple case are essentially the same as those obtained previously considering Glauber states.<sup>18</sup> However, the theory is developed in a manner which will enable the approach to be applied to other more complicated systems which would not be possible at present. Our basic results, as with the previous Glauber state results, show the factor of two discrepancy with published numerical results in strong coupling. We show how this discrepancy can be eliminated by including coupling to the upper APES.

The second aim of this paper is to apply the scale transformation to the  $E \otimes e$  problem under the assumption that the trough has been warped to produce wells. This is useful for two reasons. First, a real system is likely to be sensitive to higher-order couplings so to exhibit behavior somewhere between this case and the trough case. Secondly, the states are simpler and calculations using them somewhat more straightforward to perform as it is not necessary to integrate over all points on the trough. If good results can be obtained using this method, they will provide a quick means of writing down states for this problem and hence carrying out subsequent calculations (such as for RF's).

By applying the scale transformation, an expression for

the frequency of vibration parallel to the trough will be obtained in the limit of zero quadratic coupling, as a function of the linear coupling strength. This is shown to predict correctly the conversion of a vibration in weak coupling to a rotation in strong coupling. The ground state energy is also shown to attain the correct strong and weak coupling limits. Unfortunately, the energy is seen to be significantly overestimated in strong coupling compared to the trough results and numerical approaches.

## II. FORMULATION OF THE TROUGH PROBLEM

The linear vibronic Hamiltonian  $\mathcal{H}$  for the  $E \otimes e$  JT system contains the terms

$$\mathcal{H}_{\text{int}} = V_E \sum_i Q_i C_{E_i} \quad (1)$$

and

$$\mathcal{H}_{\text{vib+rot}} = \frac{1}{2} \sum_i \left( \frac{P_i^2}{\mu} + \mu \omega_E^2 Q_i^2 \right) C_{A_1}, \quad (2)$$

where  $i$  is summed over the components  $\theta$  and  $\epsilon$  of the  $E$  representation. The coupling constant is  $V_E$ ,  $\mu$  is the mass, and the frequency of the  $e$  mode is taken to be  $\omega_E$ .  $C_{A_1}$  is the identity operator and the  $C_{E_i}$  are electronic operators that can be represented in the matrix form

$$C_{E_\theta} = \frac{1}{2} \begin{pmatrix} 1 & 0 \\ 0 & -1 \end{pmatrix} \quad \text{and} \quad C_{E_\epsilon} = -\frac{1}{2} \begin{pmatrix} 0 & 1 \\ 1 & 0 \end{pmatrix} \quad (3)$$

with respect to basis states  $|\theta\rangle$  and  $|\epsilon\rangle$ .  $\mathcal{H}_{\text{int}}$  describes the interaction between the electrons and the vibrations and  $\mathcal{H}_{\text{vib+rot}}$  incorporates the kinetic and elastic energies for the rotational mode and the vibrational mode.

It is well-known that the lowest APES for the  $E \otimes e$  problem consists of a trough of  $O(2)$  symmetry.<sup>4</sup> This is a simple two-dimensional trough that can be represented in a plot of  $Q_\theta$  against  $Q_\epsilon$  as a circle of radius  $\rho_E$  centred on the origin. Although the formulation in terms of  $Q_\theta$  and  $Q_\epsilon$  is that traditionally used, it does not separate the rotational motion from the vibrational motion. However, such a separation can be achieved by recasting the problem in terms of ‘‘rotating’’ coordinates  $Q'_i$ . At a given point on the trough, the  $Q'_i$  are given by

$$\begin{pmatrix} Q'_\theta \\ Q'_\epsilon \end{pmatrix} = \begin{pmatrix} \cos \phi & \sin \phi \\ -\sin \phi & \cos \phi \end{pmatrix} \begin{pmatrix} Q_\theta \\ Q_\epsilon \end{pmatrix}, \quad (4)$$

where  $\phi$  is defined to be the angle between the line joining that point to the origin and the  $Q_\theta$  axis. Thus  $Q'_\epsilon$  is a rotational coordinate representing motion around the trough and  $Q'_\theta$  is a vibrational coordinate representing vibrational motion across the trough.  $\mathcal{H}_{\text{vib+rot}}$  is divided into a term  $\mathcal{H}_{\text{vib}}$  involving  $Q'_\theta$  and a term  $\mathcal{H}_{\text{rot}}$  involving  $Q'_\epsilon$ , meaning that the rotational and vibrational problems can be solved independently. The next step is to find wave functions and corresponding energies that solve the above Hamiltonians.

### A. The vibrational part

The wave functions for the vibrational problem should represent harmonic oscillators in the  $Q'_\theta$  direction (namely in the direction across the well). One method of finding such functions is to apply a unitary transformation of the form

$$U = \exp \left( i \sum_i \alpha_i P_i \right) \quad (5)$$

to the complete vibronic Hamiltonian  $\mathcal{H}$ . The effect of this transformation is to displace the origin of vibrational coordinates to positions  $\hbar \alpha_i$ . If a similar procedure were to be followed to that used to solve many different well problems previously,<sup>31–36</sup> the energy of the part of the transformed Hamiltonian  $\tilde{\mathcal{H}} = U^{-1} \mathcal{H} U$  that does not contain phonon operators would be minimized with respect to the  $\alpha_i$  using the method of Öpik and Pryce.<sup>38</sup> A set of values for the  $\alpha_i$  would be obtained that map out the bottom of the trough. The only difference here is that there are an infinite number of points at the bottom of the trough, meaning that the  $\alpha_i$  are specified in terms of the angle  $\phi$  rather than being a set of distinct values. However, an alternative procedure can be carried out by working in the rotating coordinates, replacing the  $\alpha_i$  by  $\alpha'_i$ . Although this is entirely equivalent to the original problem, the results are easier to understand. This is because in these coordinates,  $\alpha'_\theta$  must be a constant as all points on the trough are the same distance from the origin. Indeed, the value of  $Q'_\theta = \hbar \alpha'_\theta$  on the trough must be the radius of the trough,  $\rho_E$ . Performing the calculation, we find that

$$\alpha'_\theta = \frac{V_E}{2\hbar \mu \omega_E^2}. \quad (6)$$

It can be argued that  $\alpha'_\epsilon$  must be zero because this mode corresponds to a rotation, not a vibration. An alternative way of looking at this is to say that because the transformation  $U$  is applied in order to displace the origin of vibrational coordinates, it should be specified in terms of the coordinates that correspond to vibrations only. In this case,  $\alpha'_\epsilon$  is zero from the start. It should be noted that values for the  $\alpha_i$  for non-rotating coordinates can be found from  $\alpha'_\theta$  as the primed and unprimed  $\alpha_i$ 's are related in the same way as the  $Q_i$ 's in Eq. (4). Thus

$$\begin{aligned} \alpha_\theta &= \alpha'_\theta \cos \phi, \\ \alpha_\epsilon &= \alpha'_\theta \sin \phi. \end{aligned} \quad (7)$$

The energy of the minimal points on the ground and excited APES's are  $E = -E_{JT} + \frac{1}{2} \hbar \omega_E$  and  $E = 3E_{JT} + \frac{1}{2} \hbar \omega_E$ , respectively, where  $E_{JT} = V_E^2 / 8\mu \omega_E^2$  is the Jahn-Teller energy. It is useful to express this and later results in terms of the scaled coupling constant  $K_E = V_E \sqrt{\hbar / 2\mu \omega_E}$  which has the dimensions of energy. The corresponding electronic states  $|\psi_g\rangle$  on the ground APES and  $|\psi_u\rangle$  on the upper (excited) APES, expressed in terms of the fixed (unprimed) coordinates, are

$$\begin{aligned}
 |\psi_g\rangle &= \cos\left(\frac{\phi}{2}\right)|\theta\rangle - \sin\left(\frac{\phi}{2}\right)|\epsilon\rangle, \\
 |\psi_u\rangle &= \sin\left(\frac{\phi}{2}\right)|\theta\rangle + \cos\left(\frac{\phi}{2}\right)|\epsilon\rangle.
 \end{aligned} \tag{8}$$

By using Eq. (4), we can also write these results in terms of the rotating (primed) coordinates as

$$\begin{aligned}
 |\psi_g\rangle &= \cos\left(\frac{3\phi}{2}\right)|\theta'\rangle - \sin\left(\frac{3\phi}{2}\right)|\epsilon'\rangle, \\
 |\psi_u\rangle &= \sin\left(\frac{3\phi}{2}\right)|\theta'\rangle + \cos\left(\frac{3\phi}{2}\right)|\epsilon'\rangle.
 \end{aligned} \tag{9}$$

The vibronic ‘‘ground’’ states of the transformed Hamiltonian on each sheet can be written as  $|\psi_{\text{vibronic}};0\rangle$ , where  $|\psi_{\text{vibronic}}\rangle = |\psi_g\rangle$  or  $|\psi_u\rangle$  and the ‘‘0’’ indicates the absence of phonon excitations in the transformed system. States appropriate to the untransformed system can be found by multiplying these states by  $U$  after substitution of the value of  $\alpha'_\theta$ . To do this, it is useful to write  $U$  in the second quantized form  $U = \exp[k_\theta(b_\theta^{\prime\dagger} - b'_\theta)]$ , where  $k_\theta = K_E/2\hbar\omega_E$ . Note that as  $U$  contains phonon operators, there are phonon excitations present for the ground state in the untransformed system, even though they are not present in the transformed system. States with  $n$  excitations of  $\theta'$  symmetry can be obtained by multiplying the phonon vacuum state by powers of the phonon creation operator  $b_\theta^{\prime\dagger}$ . Thus the vibronic state with  $n$   $\theta'$ -type excitations can be written as

$$U|\psi_{\text{vibronic}};n\rangle = U(b_\theta^{\prime\dagger})^n|\psi_{\text{vibronic}};0\rangle. \tag{10}$$

### B. The rotational part

The terms in the Hamiltonian giving rise to rotations are the kinetic and potential energies of the  $Q'_\epsilon$  mode. In common with previous authors,<sup>3,18</sup> we will neglect the potential energy contribution. The most convenient way to find solutions for the rotational kinetic energy is to realize that  $Q'_\epsilon$  is the distance moved around the trough, so that  $dQ'_\epsilon = \rho_E d\phi$ . Consequently,

$$\mathcal{H}_{\text{rot}} = -\frac{\hbar^2}{2I} \frac{\partial^2}{\partial \phi^2} \equiv \frac{\hat{l}_z^2}{2I}, \tag{11}$$

where  $I = \mu\rho_E^2$  is the moment of inertia. This is the standard form for a rigid rotator usually quoted for the  $E \otimes e$  system.<sup>4</sup> Alternatively, the kinetic energy can be written directly in terms of  $Q'_\epsilon$  followed by a substitution of  $Q'_\epsilon = \rho_E \phi$ . Expressions can also be obtained by converting to the fixed coordinate system, using the polar parametrization  $Q_\theta = \rho_E \cos \phi$  and  $Q_\epsilon = \rho_E \sin \phi$  equivalent to Eq. (7). Expressions for the  $\partial/\partial Q_i$  can be obtained if the  $\rho_E$  is treated as a variable and then reset to a constant (and  $\partial/\partial \rho_E$  to zero). The results can then be transformed back to the rotating coordinate system,

noting that the  $P_i$  transform in the same manner as the  $Q_i$ . Whichever procedure is used, the normalized rotational wave functions will be

$$|\psi_{\text{rot}};m_j\rangle = e^{im_j\phi}/\sqrt{2\pi}. \tag{12}$$

As the electronic wave functions  $|\psi_g\rangle$  and  $|\psi_u\rangle$  contributing to the vibronic wave functions  $|\psi_{\text{vibronic}}\rangle$  change sign when  $\phi$  is incremented by  $2\pi$ , the rotational functions  $|\psi_{\text{rot}};m_j\rangle$  must also change sign for the overall wave function to be invariant. Thus it follows that  $m_j$  must be half-integer. A further discussion of this point was given by Bersuker and Polinger.<sup>4</sup>

Although the state given in Eq. (12) has a fixed value of  $m_j$ , it is sometimes more convenient (from a symmetry point of view) to define states that transform according to specific irreducible representations of the cubic group. As  $E \otimes E = E + A_1 + A_2$ , the states of the  $E \otimes e$  system must be doublets or singlets. The ground state is a doublet corresponding to the states  $m_j = \pm \frac{1}{2}$ . States transforming as the components  $E_\theta$  and  $E_\epsilon$  of the cubic group can be obtained by replacing  $e^{\pm i\phi/2}$  by  $\cos(\phi/2)$  and  $\sin(\phi/2)$ , respectively. Alternatively, they can be taken as the real and the negative of the imaginary parts respectively of the state with  $m_j = \frac{1}{2}$ .

### C. Total states

Combining the vibronic state in Eq. (10) and the rotational state in Eq. (12) gives an expression for ground and excited states at a particular point on the trough. States appropriate for the system as a whole (in non-normalized form) must involve all trough points equally via the integral

$$|\psi_{\text{tot}}^s;n,m_j\rangle = \int U|\psi_{\text{vibronic}};n\rangle|\psi_{\text{rot}};m_j\rangle d\phi \tag{13}$$

over all points  $\phi$  on the trough, where  $s = g$  or  $u$  to label the ground and upper APES's, respectively. This is equivalent to a linear sum to account mathematically for tunneling between equivalent minima in well cases. The result can be expressed in an alternative form using the commutation properties of  $b'_\theta$  with the resultant unnormalized state

$$|\psi_{\text{tot}}^s;n,m_j\rangle = e^{-(1/2)k_\theta^2} \int_0^{2\pi} e^{k_\theta b_\theta^{\prime\dagger}} (b_\theta^{\prime\dagger} - k_\theta)^n e^{im_j\phi} |\psi_s\rangle d\phi. \tag{14}$$

An equivalent expression for the ground states was obtained by Judd and Vogel,<sup>20</sup> and later by Chancey,<sup>18</sup> using generalized Glauber states. This is because when  $U$  is applied to the phonon vacuum state, the results are equivalent (up to a normalizing factor) to the expressions used when generating Glauber states. Note that these states are not exact eigenstates of  $\hat{l}_z$ , and  $\hat{l}_z$  does not commute with  $\mathcal{H}$ . Consequences of this in terms of coupling between the ground and excited potential sheets will be discussed below.

## III. ENERGIES

The energies of the resultant states can be calculated by normalizing the above states and evaluating their matrix el-



ements with respect to the untransformed Hamiltonian  $\mathcal{H}$ . When evaluating the phonon overlaps and matrix elements, it will be necessary to determine the overlaps of wave functions at two different points on the trough. As the rotating coordinates are different for the two different points, such calculations are best performed by converting back to the fixed coordinate system. All relevant overlaps can then be calculated using appropriate identities and expanding the exponentials. The same basic formulas apply here as those obtained for the overlaps and matrix elements in Ref. 39 for “well” problems, except where the two states now refer to two different points at angles  $\phi$  and  $\phi'$  on the trough rather than two different wells.

The resultant double integrals over  $\phi$  and  $\phi'$  only involve the difference in angles  $\Phi = \phi - \phi'$ , and thus can be rewritten as a single integral. Physically, the integrals arise from evaluating the overlap between two different points  $A$  and  $B$  on the trough and integrating over all possible positions of  $A$  and  $B$ . One integral can be viewed as fixing the position of point  $A$  and integrating over all possible positions of  $B$ ; this can only depend upon the difference in angles between  $A$  and  $B$ . The second integral then integrates over all possible positions of  $B$ . As all points along the trough are identical, the value of the first integral can not depend upon the position of the point  $A$ . Therefore all of the “first” integrals yield the same value and the second integral simply multiplies this value by the integral over all possible angles, namely,  $2\pi$ .

As the integrals involved in determining the overlaps and matrix elements are only single integrals, they can be evaluated numerically. Alternatively, analytical expressions for all of the resultant integrals can be obtained in terms of Bessel functions  $I_0$  and  $I_1$ . For example, for the ground state,

$$\begin{aligned} \left\langle \psi_{\text{tot}}^g; 0, \frac{1}{2} \left| \psi_{\text{tot}}^g; 0, \frac{1}{2} \right. \right\rangle &= O_1, \\ \left\langle \psi_{\text{tot}}^g; 0, \frac{1}{2} \left| \mathcal{H} \right| \psi_{\text{tot}}^g; 0, \frac{1}{2} \right\rangle &= M_1 \hbar \omega_E, \end{aligned} \quad (15)$$

where

$$\begin{aligned} O_1 &= \int_0^{2\pi} e^{K(\cos \Phi - 1)} \cos^2 \frac{\Phi}{2} d\Phi = e^{-K} \pi [I_0(K) + I_1(K)], \\ M_1 &= \int_0^{2\pi} e^{K(\cos \Phi - 1)} \cos^2 \frac{\Phi}{2} [1 + K(\cos \Phi - 2)] d\Phi \\ &= -e^{-K} \pi [(K-1)I_0(K) + KI_1(K)], \end{aligned} \quad (16)$$

where  $K = k_\theta^2 = E_{JT} / \hbar \omega_E$ . Dividing these results, we can see that the ground state energy is

$$E = \hbar \omega_E \left[ -K + \frac{I_0(K)}{I_0(K) + I_1(K)} \right]. \quad (17)$$

This expression can be seen to be exactly equivalent to that given by Chancey<sup>18</sup> if the Bessel functions are expanded as sums of polynomials.

The value of the ground state energy in Eq. (17) is plotted relative to  $-E_{JT}$  in Fig. 1 (solid line labeled “no coupling”)

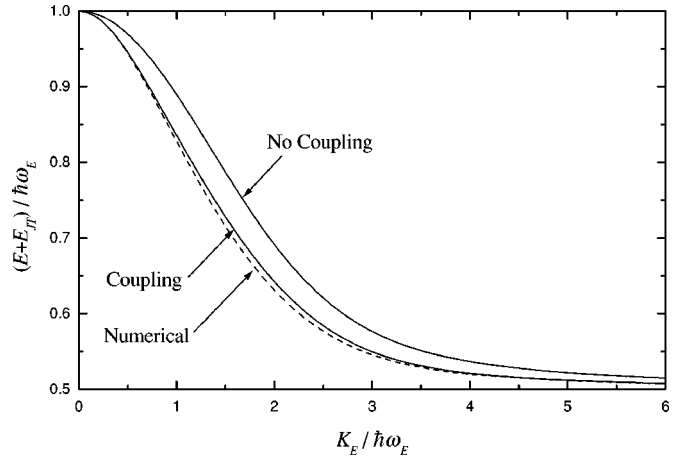


FIG. 1. The ground state energy. The solid lines give the results of the current method with and without coupling to the upper APES. The dashed line is the numerical result of Ref. 8.

as a function of the dimensionless coupling strength  $K_E / \hbar \omega_E$ . As expected, the energy at strong coupling is  $\frac{1}{2} \hbar \omega_E$ , corresponding to one vibration and one rotation. At zero coupling, the relative energy is  $\hbar \omega_E$ , representing two vibrations. This is because there is no longer a trough at zero coupling. Also plotted (dashed line) is the numerical result obtained by Longuet-Higgins *et al.*<sup>8</sup> This shows that in strong coupling, in common with the results of Chancey,<sup>18</sup> the calculated energy difference from the strong-coupling limit of  $-E_{JT} + \frac{1}{2} \hbar \omega_E$  is twice the expected value indicated by the numerical result. As noted in the introduction, this is because  $\hat{l}_z^2$  should contribute  $\hbar^2/4$  to the overall energy, whereas, due to the neglect of the rotational potential energy, it contributes twice this amount.<sup>19</sup>

The reason why  $\hat{l}_z^2$  does not contribute  $\hbar^2/4$  is that the states  $|\psi_{\text{tot}}^s; n, m_j\rangle$  contain a term  $e^{im\phi}$  from  $|\psi_{\text{rot}}; m_j\rangle$  and terms in  $\cos(\phi/2)$  and  $\sin(\phi/2)$  from the electronic states  $|\psi_s; m_j\rangle$ . Consequently, it follows that

$$\begin{aligned} \hat{l}_z^2 \left| \psi_{\text{tot}}^g; 0, \pm \frac{1}{2} \right\rangle &= \frac{\hbar^2}{2} \left( \left| \psi_{\text{tot}}^g; 0, \pm \frac{1}{2} \right\rangle \pm i \left| \psi_{\text{tot}}^u; 0, \pm \frac{1}{2} \right\rangle \right), \\ \hat{l}_z^2 \left| \psi_{\text{tot}}^u; 0, \pm \frac{1}{2} \right\rangle &= \frac{\hbar^2}{2} \left( \left| \psi_{\text{tot}}^u; 0, \pm \frac{1}{2} \right\rangle \mp i \left| \psi_{\text{tot}}^g; 0, \pm \frac{1}{2} \right\rangle \right). \end{aligned} \quad (18)$$

In other words,  $\hat{l}_z^2$  couples the ground APES to the excited APES. This observation provides a means of at least partially correcting this problem. We define a new ground state of the form

$$\left| \Phi_{\text{tot}}^g; 0, \pm \frac{1}{2} \right\rangle = \alpha \left| \Psi_{\text{tot}}^g; 0, \pm \frac{1}{2} \right\rangle \pm i \beta \left| \Psi_{\text{tot}}^u; 0, \pm \frac{1}{2} \right\rangle, \quad (19)$$

where the  $|\Psi_{\text{tot}}^s; 0, \pm \frac{1}{2}\rangle$  ( $s = u, g$ ) are normalized versions of the  $|\psi_{\text{tot}}^s; 0, \pm \frac{1}{2}\rangle$  (i.e.,  $|\psi_{\text{tot}}^s; 0, \pm \frac{1}{2}\rangle / \sqrt{O_1}$ ).  $\alpha$  and  $\beta$  are assumed to be real parameters and the factors of  $i$  are chosen for convenience.

With this definition, and noting that the normalization constants for the ground and excited electronic states are the same, we obtain

$$\hat{l}_z^2 \left| \Phi_{\text{tot}}^g; 0, \pm \frac{1}{2} \right\rangle = (\alpha + \beta) \frac{\hbar^2}{2} \left( \left| \Psi_{\text{tot}}^g; 0, \pm \frac{1}{2} \right\rangle \pm i \left| \Psi_{\text{tot}}^u; 0, \pm \frac{1}{2} \right\rangle \right). \quad (20)$$

As the overlap between the ground state on the upper APES is the same as that on the lower APES and as

$$\left\langle \psi_{\text{tot}}^g; 0, \frac{1}{2} \left| \psi_{\text{tot}}^u; 0, \frac{1}{2} \right\rangle = - \left\langle \psi_{\text{tot}}^u; 0, \frac{1}{2} \left| \psi_{\text{tot}}^g; 0, \frac{1}{2} \right\rangle = i O_2 \quad (21)$$

with

$$O_2 = \int_0^{2\pi} e^{K(\cos \Phi - 1)} \sin^2 \frac{\Phi}{2} d\Phi = e^{-K} \pi [I_0(K) - I_1(K)] \quad (22)$$

we can see that for the new state to be a (normalized) eigenstate of  $\hat{l}_z^2$ , it is necessary to set  $\alpha = \beta = 1/\sqrt{2(1 - O_2/O_1)}$ . However, the eigenvalue is  $\hbar^2/2$  rather than the expected  $\hbar^2/4$ . Furthermore, it is found that the energy ( $E + E_{JT}$ ) does not tend to a constant in strong-coupling. For the expectation value of  $\hat{l}_z^2$  to be  $\hbar^2/4$ , it is necessary to set

$$\alpha = \frac{1}{2\sqrt{2(1 - O_2/O_1)}} + \frac{\sqrt{3}}{2\sqrt{2(1 + O_2/O_1)}}, \quad (23)$$

$$\beta = \frac{1}{2\sqrt{2(1 - O_2/O_1)}} - \frac{\sqrt{3}}{2\sqrt{2(1 + O_2/O_1)}}.$$

However, ( $E + E_{JT}$ ) does not tend to a constant in strong coupling in this case either, meaning that this is not a good choice.

As  $\hat{l}_z^2$  is not the only term in the Hamiltonian, we should not concentrate on this alone. The energy of the ground state using the full Hamiltonian is given by

$$E = \frac{\alpha^2 M_1 + \beta^2 M_2 - 2\alpha\beta M_3}{(\alpha^2 + \beta^2) O_1 - 2\alpha\beta O_2}, \quad (24)$$

where  $M_2 = \langle \psi_{\text{tot}}^u; 0, \frac{1}{2} | \mathcal{H} | \psi_{\text{tot}}^u; 0, \frac{1}{2} \rangle$  and  $iM_3 = \langle \psi_{\text{tot}}^l; 0, \frac{1}{2} | \mathcal{H} | \psi_{\text{tot}}^u; 0, \frac{1}{2} \rangle$ . More explicitly,

$$M_2 = \int_0^{2\pi} e^{K(\cos \Phi - 1)} \cos^2 \frac{\Phi}{2} [1 + K(\cos \Phi + 2)] d\Phi$$

$$= e^{-K} \pi [(3K + 1)I_0(K) + 3KI_1(K)],$$

$$M_3 = \int_0^{2\pi} e^{K(\cos \Phi - 1)} \sin^2 \frac{\Phi}{2} [1 + K \cos \Phi] d\Phi$$

$$= e^{-K} \pi [(1 - K)I_0(K) + KI_1(K)]. \quad (25)$$

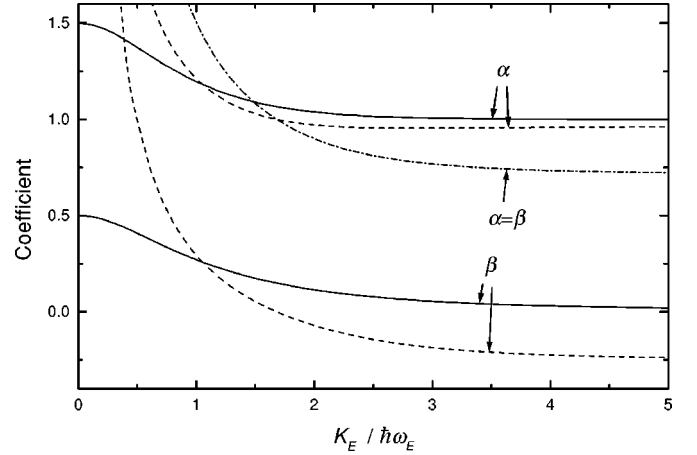


FIG. 2. The values of  $\alpha$  and  $\beta$  to minimize the energy of the ground state (solid lines), for the ground state to be an eigenstate of  $\hat{l}_z^2$  (dot-dash line) and for  $\hat{l}_z^2$  to have an expectation value of  $\hbar^2/4$  (dashed line).

We therefore choose to minimize the energy in Eq. (24) by setting  $dE/d\alpha = 0$  and  $dE/d\beta = 0$  and choosing the root that gives the lowest energy. Thus, after some simple algebra, we obtain the result  $\alpha = l\beta$ , where

$$l = \frac{(M_2 - M_1)O_1 + \sqrt{x}}{2(M_3O_1 - M_1O_2)} \quad (26)$$

and

$$x = (M_2 - M_1)^2 O_1^2 - 4(M_3 O_1 - M_1 O_2)(M_2 O_2 - M_3 O_1). \quad (27)$$

The condition that the state is normalized fixes the absolute values of  $\alpha$  and  $\beta$  (up to the usual phase factor) so that

$$\beta = 1/\sqrt{(l^2 + 1) - 2lO_2/O_1} \quad (28)$$

These values of  $\alpha$  and  $\beta$  are plotted as a function of coupling strength as solid lines in Fig. 2. The figure also shows the results for the state to be an eigenstate of  $\hat{l}_z^2$  (dot-dash line) and for  $\hat{l}_z^2$  to have an expectation value of  $\hbar^2/4$  (dashed lines). The energy of the ground state determined using the variational values for  $\alpha$  and  $\beta$  is shown in Fig. 1 (solid line labeled “coupling”). It can be seen that the new result is very close to the numerical result<sup>8</sup> for all coupling strengths. In particular, the value in strong coupling is halved from that when the coupling is neglected.

In the strong-coupling limit,  $O_2$  and  $M_3 \rightarrow 0$ , implying no mixing of the state on the upper APES into the ground state. The results above give  $\alpha \rightarrow 1$  and  $\beta \rightarrow 0$  in this limit, which is consistent with this observation. This behavior is also to be expected because the original energies were seen to be correct in this limit; it is only the rate at which the limiting values of energy were obtained that was incorrect. Note also that because the electronic states on the ground and upper potential sheets are orthogonal to each other, the energies of the new states with  $m_j = \pm \frac{1}{2}$ , or equivalently of the  $E_\theta$  and  $E_\epsilon$  components, are still the same as each other.

It should be noted that although we have used a variational procedure to determine the amount of mixing of the ground state on the upper APES into the ground state on the lower APES, the ground states on the APES's are not themselves of a variational nature. The wave functions are of a totally different form to those used in other variational calculations in which the wave functions themselves are variational.<sup>24-27</sup> It should also be noted that the overlap factors and matrix elements between the  $m_j = +1/2$  and  $m_j = -1/2$  states are zero. As corresponding  $m_j = +1/2$  and  $m_j = -1/2$  states are degenerate at all coupling strengths, it is possible to define states composed of any linear combination of the lowest  $m_j = +1/2$  and  $m_j = -1/2$  states on each APES. However, the energy of the resultant state after minimizing the energy with respect to the variational parameters will be the same in all of these cases.

We will now derive results for the excited vibrational and rotational states. It is again found necessary to include coupling to the upper APES. The coupling still roughly halves the difference between the calculated result and  $E_{JT} + \frac{1}{2}\hbar\omega_E$ , although the effect is even more noticeable than for the ground states because the magnitude of the reduction is much larger. It should be noted that the overlap integrals for many of the excited states tend to zero in the weak-coupling limit, meaning that the states themselves are not properly defined in this limit. This is not surprising as we have used a picture involving rotations around a trough and vibrations across a trough. There is no trough in the weak coupling limit and so this is not appropriate. Nevertheless, because the matrix elements also tend to zero, the energy does attain a well-defined finite limit. Unfortunately, the energies of the higher angular momentum states with phonon excitations tend to the wrong limit. This is illustrated in Fig. 3 for the  $m_j = \pm\frac{7}{2}$  states with one phonon excitation. The dot-dash and dotted lines are the results with and without coupling to the excited APES, respectively. It can be seen that both results tend to  $4\hbar\omega_E$  in weak coupling rather than the correct value of  $5\hbar\omega_E$  ( $\hbar\omega_E$  zero-point energy for two vibrations,  $\hbar\omega_E$  for the one-phonon excitation plus  $3\hbar\omega_E$  corresponding to the  $m_j = \frac{7}{2}\hbar\omega_E$  rotation becoming a three-phonon vibration).

The occurrence of wrong limits in weak coupling has occurred before in other systems with wells in the APES.<sup>40</sup> As in these other systems, the problem arises because basis states with the same value of  $m_j$  but different phonon occupations are not orthogonal to each other. The effect is subtle because the overlap between the no-phonon and one-phonon states actually tends to zero in weak coupling, but this is a consequence of the fact that the states are poorly defined in this limit. Nevertheless, the problem can be corrected by defining new states that are orthogonal to all lower-energy states with the same value of  $m_j$ . The only drawback to this procedure is that more integrals are required and the results are inevitably more complex, although all integrals can still be reduced to a single dimension. The result with both coupling to the excited APES and orthogonalization is given as a solid line in Fig. 3, showing that the correct weak-coupling behavior is now obtained. This is despite the fact that we are working with a strong-coupling model. The  $m_j = \pm\frac{1}{2}$  states

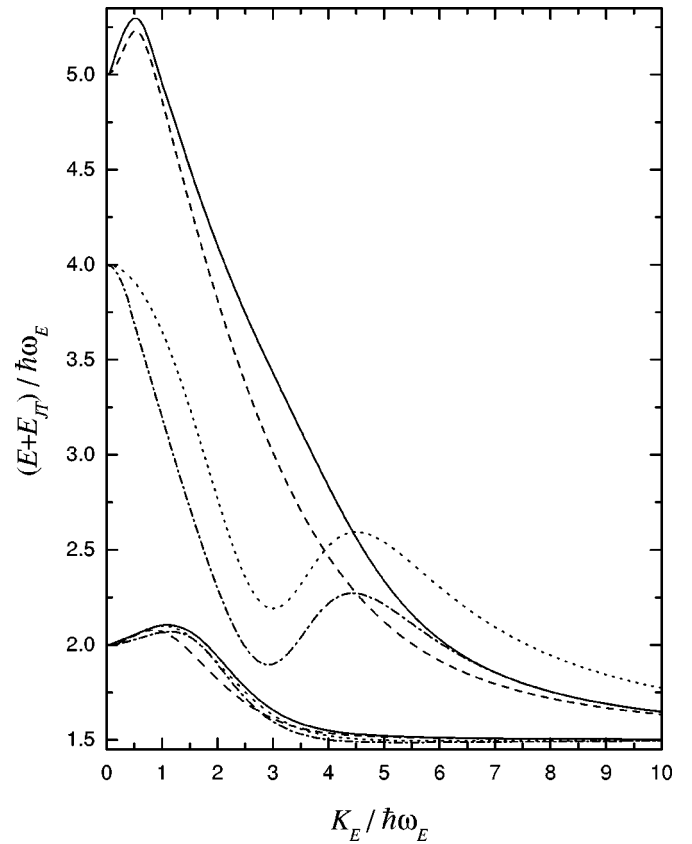


FIG. 3. The energies of the  $m_j = \pm\frac{1}{2}$  and  $\pm\frac{7}{2}$  states with one phonon excitation. The solid lines are the results with both orthogonalization and coupling to the upper APES. The dot-dash and dotted lines are the results before orthogonalization, with and without coupling to the excited APES respectively. The dashed lines are the numerical results of Ref. 8.

are also given in Fig. 3. This shows that orthogonalization can be included for these states also, but it does not have a significant effect on the results. Comparison with published numerical results<sup>8</sup> (dashed lines) show good agreement with the fully corrected states, although there remains some discrepancy in intermediate coupling. This is the hardest region to model both analytically and numerically.

Figure 4 gives the energies, including orthogonalization and coupling to the upper APES (solid lines) for all of the  $m_j = \pm\frac{1}{2}, \pm\frac{3}{2}, \pm\frac{5}{2},$  and  $\pm\frac{7}{2}$  states (in order of increasing energy) for phonon occupation numbers of 0, 1, and 2. The ground state given in Fig. 1 and the one-phonon states given in Fig. 3 are included again for completeness. In strong coupling, the rotational levels can clearly be seen to be structure superimposed upon phonon states separated by the vibrational quanta  $\hbar\omega_E$ . In weaker couplings, the states with higher  $m_j$  values start to cross states with lower  $m_j$  values but an additional phonon excitation, until the weak coupling limit where all states are separated by the vibrational quantum  $\hbar\omega_E$ . The numerical results of Longuet-Higgins *et al.*<sup>8</sup> are also shown (as dashed lines). It can be seen that the agreement for all of the zero-phonon states is excellent. The agreement becomes less good as the number of phonon excitations increases, in common with the observation above.

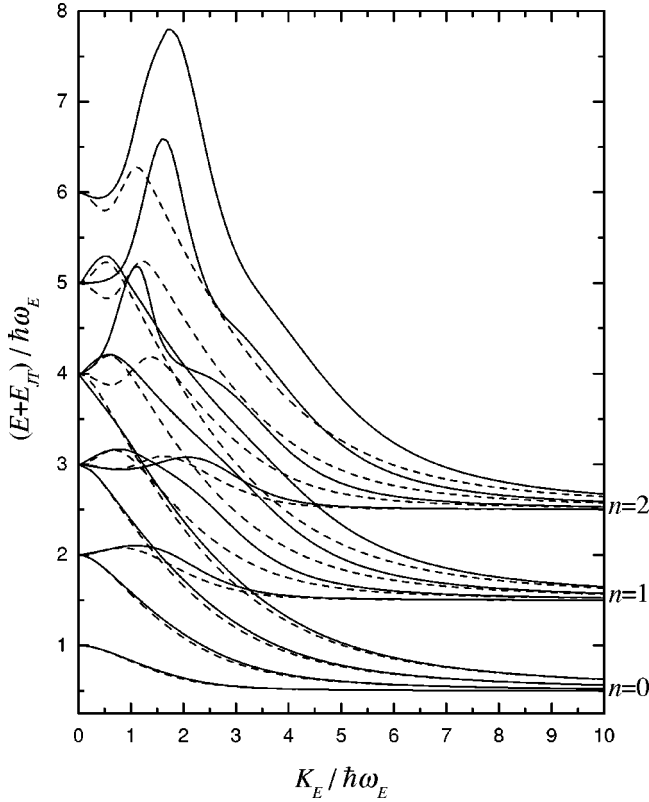


FIG. 4. The energies of the states with  $m$  of  $\pm\frac{1}{2}$ ,  $\pm\frac{3}{2}$ ,  $\pm\frac{5}{2}$ , and  $\pm\frac{7}{2}$  (in order of increasing energy, respectively) for phonon occupation numbers  $n$  of 0, 1, and 2. The solid lines give the results of the current method including coupling to the upper sheet and the dashed lines are the numerical results of Ref. 8.

#### IV. THE ANISOTROPIC WELL PROBLEM

The results of the trough problem should be compared with those of the equivalent problem that arises when quadratic coupling is included to warp the lowest APES into three equivalent wells via a term such as

$$\mathcal{H}_{\text{quad}} = V_2[(Q_\epsilon^2 - Q_\theta^2)C_{E_\theta} + 2Q_\epsilon Q_\theta C_{E_\epsilon}], \quad (29)$$

where  $V_2$  is a quadratic coupling constant. It is not expected that the two approaches will produce equivalent results as they model different physical situations; whereas the trough states include an infinite set of points at the bottom of the trough, the well problem includes three points only. Nevertheless, comparison of the two approaches can indicate how a real system with a small amount of quadratic coupling will behave.

The wells in the lowest APES, which will be labeled  $A$ ,  $B$ , and  $C$ , correspond to the points

$$\phi/2=0, \quad 2\pi/3, \quad \text{and} \quad 4\pi/3, \quad (30)$$

respectively in Eq. (8) for the ground and excited electronic states on the trough. Symmetrized combinations of the well states taken to allow for tunneling between the wells in finite coupling yield expressions for the ground doublet state (of  $E$  symmetry), and also a singlet tunneling level (of  $A_2$  symmetry).<sup>33</sup>

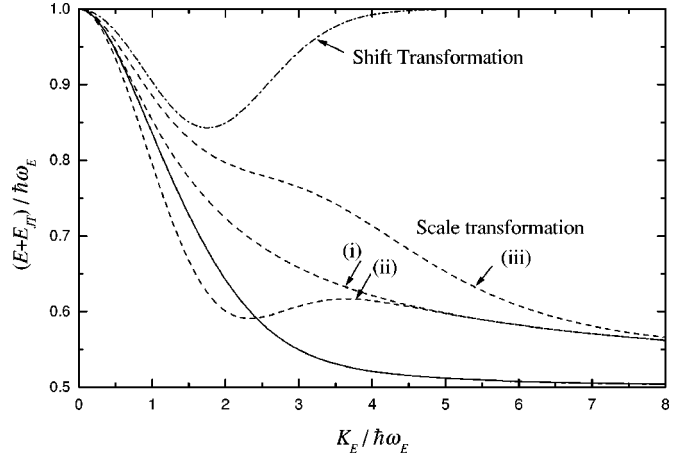


FIG. 5. Comparison of the ground state energy using trough and well states. The solid line is the ground state of the trough method as given in Fig. 1. The dot-dash line is the results of calculations based on isotropic well states when the quadratic coupling tends to zero. The dashed line labeled (i) is the well energy corrected for anisotropy, line (ii) is the ground state energy using the corrected well energy but with all other terms as for the isotropic result, and line (iii) is the ground state energy calculating all terms to first order and including anisotropy.

Often, in order to simplify well problems, the wells are taken to be isotropic. However, this will not be a good approximation for the  $E \otimes e$  JT system as the barriers in the direction around the trough will be much lower than across the trough, and the corresponding vibrational frequency will be less. Furthermore, the results cannot reproduce the trough results in the limit when the quadratic coupling tends to zero. This is shown in Fig. 5 (dot-dash line). The state starts at the correct energy in weak coupling and begins to reduce as the (linear) coupling strength increases. However, it then starts to increase again and ends  $\frac{1}{2}\hbar\omega_E$  too large in the strong coupling limit. This is because the rotation that should take place around the trough is effectively still treated as a vibration, bringing with it its zero-point energy.

Better results for the well problem can be obtained by incorporating anisotropy in the wells. Values of the anisotropic local mode frequencies in the limit of strong linear coupling can be obtained using the method of Öpik and Pryce,<sup>38</sup> as applied previously for the icosahedral  $T_{1u} \otimes h_g$  system.<sup>41</sup> First, the curvature of the APES is analyzed by expanding the potential energy  $V(Q)$  to second order as a power series about each minimum. In general terms, if a minimum  $k$  has coordinates  $Q^{(k)} \equiv \{Q_i^{(k)}\}$ , the required potential is

$$V(q) = V(Q^{(k)}) + V_1(q) + V_2(q), \quad (31)$$

where<sup>41</sup>

$$V_1(q) = \sum_i \left( \frac{\partial V}{\partial Q_i} \right)_{Q^{(k)}} q_i,$$



$$V_2(q) = \frac{1}{2} \sum_i \sum_j \left( \frac{\partial^2 V}{\partial Q_i \partial Q_j} \right)_{Q^{(k)}} q_i q_j, \quad (32)$$

and  $q_i = Q_i - Q_i^{(k)}$  are the nuclear displacements from the minimum  $k$ .

In this problem, the potential  $V(Q)$  is

$$V(Q) = \sum_{i=\theta,\epsilon} \left( \frac{1}{2} \mu \omega_E^2 Q_i^2 + V_E Q_i C_{E_i} \right). \quad (33)$$

The zeroth order term  $V(Q^{(k)})$  is that used to determine the positions of the wells, and is therefore known to give the energy  $-E_{JT}$ . This can also be seen by substituting the appropriate values of  $Q_i^{(k)} = -\alpha_i \hbar$  for a given well  $k$ . The values of  $\alpha_i$  for zero quadratic coupling can be obtained from Eq. (7) by substituting the values of  $\phi$  for the well positions given in Eq. (30). In finite quadratic coupling, both the values of  $\alpha_i$  and the Jahn-Teller energy are multiplied by  $1/(1-L)$ , where  $L = |V_2|/\mu\omega_E^2$ .<sup>35</sup> Thus it can be seen that the warping has a small effect upon these parameters. Hence in the following calculations,  $V_2$  will be set to zero, even though there are not actually wells in this case and the continuous trough description should be used. The remaining terms in Eq. (31) can then be used to determine the energy of well  $k$  to second-order in perturbation theory (in the limit of zero quadratic coupling). There are no linear terms in  $q_i$  as  $V(q)$  is a minimum at  $Q_i = Q_i^{(k)}$ . Therefore, the energy may be written in the form

$$E(q) = -E_{JT} + \frac{1}{2} (q_\theta q_\epsilon) M \begin{pmatrix} q_\theta \\ q_\epsilon \end{pmatrix}, \quad (34)$$

where  $M$  is a  $2 \times 2$  matrix. This matrix defines the curvature of the energy surface. In general, the eigenvalues of  $M$  are of the form  $\mu\omega_n^2$ , where the  $\omega_n$  are the frequencies of the local modes. In this case, the matrix for well  $A$  is

$$M_A = \mu\omega_E^2 \begin{pmatrix} 1 & 0 \\ 0 & 0 \end{pmatrix} \quad (35)$$

so it is immediately clear that the local mode frequencies in the infinite coupling limit are  $\omega_E$  and 0. This is consistent with the view of a vibration of frequency  $\omega_E$  across the trough and a rotation around the trough. For well  $B$ , the  $M$  matrix is

$$M_B = \frac{1}{4} \mu\omega_E^2 \begin{pmatrix} 1 & \sqrt{3} \\ \sqrt{3} & 3 \end{pmatrix}. \quad (36)$$

This matrix may be diagonalised using the unitary matrix

$$S_B = \frac{1}{2} \begin{pmatrix} 1 & \sqrt{3} \\ \sqrt{3} & -1 \end{pmatrix} \quad (37)$$

again giving the local mode frequencies  $\omega_E$  and 0.

In finite linear coupling, the local mode frequencies are not simply  $\omega_E$  and 0 but exhibit a complicated dependence upon the coupling strength. The results must predict two vibrations in the weak coupling limit as well as a vibration and

a rotation in the strong-coupling limit. Finite-coupling local mode frequencies can be obtained by applying a scale transformation<sup>37</sup>

$$U_s = \exp \left[ \sum_{i,j} \Lambda_{ij} (b_i b_j - b_i^\dagger b_j^\dagger) \right] \quad (38)$$

in addition to the shift transformation.  $\Lambda_{ij}$  is an element of a matrix  $\Lambda$  which, similar to the parameters  $\alpha_i$  in the shift transformation will be set to minimize the energy. The effect of this transformation is to both transform to a new coordinate system and to scale the new coordinates by different amounts. This can be seen by noting that the zeroth-order wave functions are a product of simple-harmonic oscillator functions of the form

$$\psi(Q_i) \sim \exp \left( -\frac{\mu\omega_E}{\hbar} Q_i^2 \right). \quad (39)$$

It can be shown that the effect of the diagonal elements  $U_s^{ii}$  of the scale transformation on such a wave function is

$$U_s^{(ii)} \psi(Q_i) \sim e^{\Lambda_{ii}} \psi(e^{2\Lambda_{ii}} Q_i). \quad (40)$$

Therefore, if we choose  $\Lambda_{ii} = \frac{1}{4} \ln \lambda_i$ ,

$$U_s^{(ii)} \psi(Q_i) \sim \lambda_i^{1/4} \exp \left( -\frac{\mu\omega_i}{\hbar} Q_i^2 \right), \quad (41)$$

where  $\lambda_i = \omega_i/\omega_E$  is the ratio of the scaled to unscaled frequencies. Thus the original isotropic frequencies are replaced by new scaled frequencies.

Now overall, it is desired that the complete matrix  $e^{2\Lambda}$  in Eq. (40) formed from the scale transformation parameters  $\Lambda_{ij}$  should not only scale the new coordinates but also transform the basis vectors  $Q_i$  to the directions of the local modes. These are the eigenvectors of the curvature matrix  $M$  in Eq. (34). The matrices to achieve this are the  $S$  matrices such as Eq. (37) already obtained using the Öpik and Pryce method to obtain the strong-coupling frequencies. In fact, the  $S$  matrices have this effect on all matrices  $e^{\pm n\Lambda}$ . Therefore, combining this information with the requirement for the diagonal elements to scale the frequencies indicates we should choose

$$\Lambda = \frac{1}{4} S^\dagger [\ln \lambda_i] S, \quad (42)$$

where  $[\ln \lambda_i]$  is a square diagonal matrix with elements  $(\ln \lambda_i)$ .<sup>37,41</sup> We then have

$$e^{\pm n\Lambda} = S^\dagger [\lambda_i^{\pm n/4}] S. \quad (43)$$

Note that the  $S$  matrices can also be deduced using other methods such as projection operators or the so-called eigenfunction method.<sup>41,42</sup>

The next step is to determine values for finite-coupling local mode frequencies by fixing values for the scale transformation parameters by energy minimization (as for the shift transformation parameters). This involves finding the effect of the scale transformation on the transformed Hamil-

tonian. The part of  $\tilde{\mathcal{H}}$  that does not contain phonon operators is the same as with the shift transformation alone except for the addition of the term

$$\hbar\omega_E \sum_i (\sinh 2\Lambda)_{ii}^2, \quad (44)$$

where the effect of the operator  $\sinh 2\Lambda$  can be determined by converting to exponential notation and using the definition in Eq. (43). Unfortunately, if we use the zeroth order states and include this term alone, we find the correction to the ground state well energy  $-E_{JT} + \hbar\omega_E$  is

$$\frac{\hbar\omega_E}{4} \left( \lambda_1 + \frac{1}{\lambda_1} + \lambda_2 + \frac{1}{\lambda_2} - 4 \right). \quad (45)$$

Minimizing the corrected energy with respect to the  $\lambda_i$  simply gives  $\lambda_1 = \lambda_2 = 1$ , which is the isotropic result. This is not a surprising result as anisotropy is a second-order effect. We must therefore calculate the energy to second-order in perturbation theory. The dominant effect will be from states with one phonon excitation, which are coupled to the ground state via the transformed Hamiltonian

$$\tilde{\mathcal{H}}_2 = \sum_{ij} \left( -K_E C_{E_i} + \frac{1}{2} \hbar\omega_E \sqrt{2\hbar\mu\omega_E\alpha_i} \right) (b_j + b_j^\dagger) e_{ji}^{-2\Lambda}. \quad (46)$$

One-phonon states on both the lowest APES and the excited APES will be coupled by this Hamiltonian, and both possibilities should be included.

The easiest calculation is for the well *A* as  $S_A$  is the identity matrix and  $e^{-2\Lambda}$  is diagonal, although the same results are obtained whichever well is used. Evaluating the appropriate matrix elements, we find that the correction to the ground state well energy now contains the additional contribution  $-E_{JT}/\{\lambda_2[1+4E_{JT}/(\hbar\omega_E)]\}$ . Minimizing all of the energy contributions with respect to the  $\lambda_i$  then gives  $\lambda_1 = 1$  and

$$\lambda_2^2 = 1 - \left( 1 + \frac{\hbar\omega_E}{4E_{JT}} \right)^{-1}. \quad (47)$$

This has the correct properties of tending to 1 in weak coupling (for a vibration) and 0 in strong coupling (for a rotation). This also leads to the result

$$E = -E_{JT} + \frac{1}{2} \hbar\omega_E (1 + \lambda_2), \quad (48)$$

giving a zero-point energy of  $\hbar\omega_E$  in weak coupling and  $\frac{1}{2}\hbar\omega_E$  in strong coupling, again consistent with conversion of a vibration to a rotation.

As the energy has been corrected to second order, it is also necessary to include perturbation corrections to the well states. For well *A*, the result to first order is

$$|A\rangle = |\theta; 0\rangle - \frac{K_E}{2\sqrt{\lambda_2}(4E_{JT} + \hbar\omega_E)} |\epsilon; \epsilon\rangle, \quad (49)$$

where  $|\epsilon; \epsilon\rangle$  denotes an electronic state  $|\epsilon\rangle$  coupled to a phonon excitation of symmetry  $\epsilon$ . Equivalent results for the other wells are obtained when  $\theta$  and  $\epsilon$  are replaced by the appropriate combinations of  $\theta$  and  $\epsilon$  in Eq. (8). Coupling to states with two phonon excitations may be included also, but this vastly complicates the calculations.

The final step is now to calculate the new energy of the symmetry-adapted ground state built from these new well states. The principle of the calculation of the overlaps and matrix elements of the untransformed Hamiltonian between these corrected states is the same as that given in Badran and Bates,<sup>33</sup> although the details are considerably more complicated as they involve operating with matrices such as Eq. (43). Therefore, it is first useful to note that the matrix element within any of the wells, called  $E_{11}$  in Ref. 33, is simply the energy given in Eq. (48). This is shown as the dashed line labeled (i) in Fig. 5. An approximate expression for the ground state energy can therefore be obtained quite simply by replacing  $E_{11}$  in Eq. (3.8) of Ref. 33 for the isotropic result by the energy in Eq. (48). This is shown as the dashed line labeled (ii), together with the ground state energy using the trough states as given in Fig. 1 (solid line). It can be seen that both the well energy in Eq. (48) and the new zeroth order ground state energy attain the correct limits in both strong and weak coupling, unlike the isotropic result which is  $\frac{1}{2}\hbar\omega_E$  too large in strong coupling. This confirms that the vibration has correctly converted to a rotation. The new ground state energy is also quite close to the trough result for weaker couplings. However, the energies tend to  $\frac{1}{2}\hbar\omega_E$  far too slowly in strong coupling. We therefore complete the calculation of the energies to first-order using the well states in Eq. (48) to see if there is any improvement in the strong-coupling results.

It is found that, to first order, the overlap between the states in any two wells (which are all the same as each other) becomes

$$S_{12} = S_{12}^{(0)} (1 + F_{12}^{(1)}), \quad (50)$$

where

$$S_{12}^{(0)} = -2 \sqrt{\frac{\lambda_2}{(3+\lambda_2)(1+3\lambda_2)}} \exp\left(-\frac{6E_{JT}\lambda_2}{(1+3\lambda_2)\hbar\omega_E}\right) \quad (51)$$

is the zeroth order anisotropic phonon overlap and

$$F_{12}^{(1)} = \frac{12E_{JT}}{(4E_{JT} + \hbar\omega_E)(1+3\lambda_2)}. \quad (52)$$

The zeroth order anisotropic matrix element between any two wells is

$$E_{12}^{(0)} = \frac{4S_{12}^{(0)}}{(1+3\lambda_2)} \left[ -E_{JT} \frac{(1+6\lambda_2+3\lambda_2)^2}{(1+3\lambda_2)} + \hbar\omega_E \frac{(1+\lambda_2)^2}{(3+\lambda_2)} \right] \quad (53)$$

and the first-order contribution is

$$E_{12}^{(1)} = \frac{4S_{12}^{(0)}F_{12}^{(1)}}{(1+3\lambda_2)} \left[ E_{JT} \frac{(1-3\lambda_2^2)}{(1+3\lambda_2)} + \hbar\omega_E \frac{(7+9\lambda_2)}{3(3+\lambda_2)} \right]. \quad (54)$$

Using Eq. (3.8) of Ref. 33, after noting that the original orbital overlap of  $-\frac{1}{2}$  must be substituted by the new overlap, we obtain the ground state energy from

$$E = \frac{E_{11} - E_{12}}{1 - S_{12}}. \quad (55)$$

Figure 5 shows this energy [dashed line labeled (iii)]. It can be seen that, rather than reducing the difference between the trough result and the approximate anisotropic well result, the difference has increased. The strong-coupling behavior is clearly dominated by the well energy  $E_{11}$ . It can be surmised that the strong-coupling behavior cannot be improved further unless the well energy is improved. It is not clear whether better results could ever be obtained from this approach because the states obtained still only consider specific points on the trough. One possible improvement would be to correct the states to include coupling to states with two phonons, and then obtain the corrected energies accordingly. However, the calculation then becomes extremely cumbersome. The whole idea of obtaining a result from well states is that the calculation is relatively simple and avoids having to evaluate integrals as arise in the trough problem. Therefore this modification will not be attempted here. We can conclude that the points that become wells when quadratic coupling is included are the most important ones, and that these points alone can be used to give an indication of the true results without performing any integrations. However, it seems that more accurate results can only be obtained by solving the full trough problem.

## V. CONCLUSIONS

In this paper, we have obtained results for the linear  $E \otimes e$  system in which the lowest APES forms a trough and the motion is composed of a vibration across the trough and a rotation around the trough. We have also obtained results for the related system in which the trough is approximated by

only the three points that become minimum points when quadratic coupling is included to warp the APES. The resultant motion is then composed of a vibration across the trough and a lower-frequency vibration around the trough. A real system is likely to possess shallow barriers in the trough direction, which will result in a hindered rotation around the trough. It has been seen that the results of the two different methods are remarkably similar, considering that the two approaches are not expected to yield the same results in the limit of zero quadratic coupling as the former (correctly) includes all points on the trough whereas the latter only includes the three well points. This gives us confidence that we can predict the behavior of real systems.

It is instructive to comment on the relative merits of the two approaches. The trough approach leaves us with more physical feeling for the behavior observed than with approaches that are numerical from the outset, and yields states that can be written down analytically in terms of integrals. The results agree well with existing numerical results.<sup>8</sup> However, the integrals obtained must be either evaluated numerically or expressed analytically in terms of Bessel functions or other rather complicated infinite series. This means that some of the advantages of an analytical approach are lost. The latter approach yields more concise analytical results; it is only necessary to use a computer to graphically display the final formula. However, the calculation of the required overlaps and matrix elements is complicated by the necessary inclusion of anisotropy, and the method can never properly include the rotation as only three points are included.

The  $E \otimes e$  system has been chosen as the subject of this paper because existing results are well known, making it an ideal testing ground for new methods. These methods can then be applied to other systems where results are either not known or difficult to obtain by existing methods. This is particularly true of the trough approach, which unlike existing methods can be applied to troughs of higher dimensions.

## ACKNOWLEDGMENTS

M.R.E. would like to thank the University of Nottingham for a research studentship.

<sup>1</sup>F.S. Ham, Phys. Rev. **138**, A1727 (1965).

<sup>2</sup>F.S. Ham, *Electron Paramagnetic Resonance*, edited by S. Geschwind (Plenum, New York, 1972), pp. 1–119.

<sup>3</sup>M.C.M. O'Brien, Phys. Rev. **187**, 407 (1969).

<sup>4</sup>I. B. Bersuker and V. Z. Polinger, *Vibronic Interactions in Molecules and Crystals* (Springer, Berlin, 1989), pp. 25–28.

<sup>5</sup>Yu.E. Perlin and M.H.L. Wagner, *The Dynamical Jahn-Teller Effect in Localized Systems* (North Holland, Amsterdam, 1984).

<sup>6</sup>V.Z. Polinger, C.A. Bates, and J.L. Dunn, J. Phys.: Condens. Matter **3**, 513 (1991).

<sup>7</sup>Y.M. Liu, J.L. Dunn, and C.A. Bates, J. Phys.: Condens. Matter **6**, 859 (1994).

<sup>8</sup>H.C. Longuet-Higgins, U. Öpik, M.H.L. Pryce, and R.A. Sack, Proc. R. Soc. London, Ser. A **244**, 1 (1958).

<sup>9</sup>M.S. Child and H.C. Longuet-Higgins, Philos. Trans. R. Soc. London, Ser. A **254**, 259 (1961).

<sup>10</sup>M.C.M. O'Brien and S.N. Evangelou, J. Phys. C **13**, 611 (1980).

<sup>11</sup>A. Thiel and H. Köppel, J. Chem. Phys. **110**, 9371 (1999).

<sup>12</sup>K.A. Bosnick, Chem. Phys. Lett. **317**, 524 (2000).

<sup>13</sup>N. Manini and E. Tosatti, Phys. Rev. B **58**, 782 (1998).

<sup>14</sup>H. Koizumi and I.B. Bersuker, Phys. Rev. Lett. **83**, 3009 (1999).

<sup>15</sup>C.P. Moate, M.C.M. O'Brien, J.L. Dunn, C.A. Bates, Y.M. Liu, and V.Z. Polinger, Phys. Rev. Lett. **77**, 4362 (1996).

<sup>16</sup>P. DeLosRios, N. Manini, and E. Tosatti, Phys. Rev. B **54**, 7157 (1996).

<sup>17</sup>B.R. Judd, J. Chem. Phys. **67**, 1174 (1977).

<sup>18</sup>C.C. Chancey, J. Phys. A **17**, 3183 (1984).

<sup>19</sup>B.R. Judd, Can. J. Phys. **52**, 999 (1974).

- <sup>20</sup>B.R. Judd and E.E. Vogel, *Phys. Rev. B* **11**, 2427 (1975).
- <sup>21</sup>H. Barentzen, G. Olbrich, and M.C.M. O'Brien, *J. Phys. A* **14**, 111 (1981).
- <sup>22</sup>J. Rivera-Iratchet, A.A. de Orúe, M.L. Flores, and E.E. Vogel, *Phys. Rev. B* **47**, 10 164 (1993).
- <sup>23</sup>J. Rorison and M.C.M. O'Brien, *J. Phys. C* **17**, 3449 (1984).
- <sup>24</sup>J.R. Fletcher, *J. Phys. C* **5**, 852 (1972).
- <sup>25</sup>H. Zheng and K.-H. Bennemann, *Solid State Commun.* **91**, 213 (1994).
- <sup>26</sup>W.H. Wong and C.F. Lo, *Phys. Lett. A* **223**, 123 (1996).
- <sup>27</sup>P. Huai and H. Zheng, *Phys. Lett. A* **240**, 341 (1998).
- <sup>28</sup>H.G. Reik and M. Doucha, *Chem. Phys. Lett.* **127**, 413 (1986).
- <sup>29</sup>J.R. Fletcher and G.E. Stedman, *J. Phys. C* **17**, 3441 (1984).
- <sup>30</sup>E. E. Vogel, Ph.D. thesis, The John Hopkins University, 1975.
- <sup>31</sup>C.A. Bates, J.L. Dunn, and E. Sigmund, *J. Phys. C* **20**, 1965 (1987).
- <sup>32</sup>L.D. Hallam, J.L. Dunn, and C.A. Bates, *J. Phys.: Condens. Matter* **4**, 6775 (1992).
- <sup>33</sup>R.I. Badran and C.A. Bates, *J. Phys.: Condens. Matter* **3**, 6329 (1991).
- <sup>34</sup>R.I. Badran, S. Jamila, P.J. Kirk, C.A. Bates, and J.L. Dunn, *J. Phys.: Condens. Matter* **5**, 1505 (1993).
- <sup>35</sup>S. Jamila, J.L. Dunn, and C.A. Bates, *J. Phys.: Condens. Matter* **5**, 1493 (1993).
- <sup>36</sup>J.L. Dunn and C.A. Bates, *Phys. Rev. B* **52**, 5996 (1995).
- <sup>37</sup>Y.M. Liu, C.A. Bates, J.L. Dunn, and V.Z. Polinger, *J. Phys.: Condens. Matter* **8**, L523 (1996).
- <sup>38</sup>U. Öpik and M.H.L. Pryce, *Proc. R. Soc. London, Ser. A* **238**, 425 (1957).
- <sup>39</sup>J.L. Dunn, *J. Phys. C* **21**, 383 (1988).
- <sup>40</sup>J.L. Dunn, *J. Phys.: Condens. Matter* **1**, 7861 (1989).
- <sup>41</sup>Y.M. Liu, J.L. Dunn, C.A. Bates, and V.Z. Polinger, *J. Phys.: Condens. Matter* **9**, 7119 (1997).
- <sup>42</sup>J.-Q. Chen and M.-J. Gao, *J. Math. Phys.* **23**, 928 (1992).